



Innovative ceramic hollow fiber membranes for recycling/reuse of oilfield produced water

Mehrdad Ebrahimi^{a,b,*}, Steffen Kerker^{a,b}, Sven Daume^a, Morgan Geile^a, Frank Ehlen^c, Ina Unger^c, Steffen Schütz^c, Peter Czermak^{a,d}

^a*Institute of Bioprocess Engineering and Membrane Technology, University of Applied Sciences Mittelhessen, Gießen, Germany, email: mehrdad.ebrahimi@kmub.thm.de (M. Ebrahimi)*

^b*ehc-memtec UG, Gießen, Germany, email: info@ehc-memtec.de (S. Kerker)*

^c*MANN+HUMMEL GmbH, Ludwigsburg, Germany*

^d*Department of Chemical Engineering, Kansas State University, Manhattan KS, USA*

Received 30 April 2014; Accepted 16 June 2014

ABSTRACT

The focus of this study was on the development and application of ceramic hollow fiber membrane (CHFMs) technology for the treatment of oilfield produced water (PW) prior to disposal/discharge into the environment. PW refers to any fossil water that is brought to the surface along with crude oil or natural gas. It is a complex mixture of dispersed oil, dissolved organic compounds, suspended solids, production chemicals, heavy metals, and natural radioactive minerals. PW is difficult to handle/treat and represents the largest volume of waste associated with the oil and gas industry. It can have different potential impacts on offshore or onshore environments depending on where it is discharged. Therefore, the development of effective treatment technologies for PW is essential from both ecological and economic standpoints. The first stage of any treatment process for PW consists of a significant reduction in the level of dispersed hydrocarbons and suspended solids. In a second and often in a third stage, the oil and total carbon (TC) content is reduced by hydrocyclones and by micro- and ultrafiltration using membrane technologies. Due to legal requirements, final oil contents below 10 ppm are required in some regions before PW disposal to the environment. CHFMs represent a new generation in the development of inorganic membranes by offering the advantages of one membrane consisting of both inorganic material and hollow fiber geometry. In this study, the effect of cross-flow velocity on the CHFMs performance at a low trans-membrane pressure of 0.5 bar, as well as the permeate quantity and quality, was investigated in terms of fouling behavior and efficiency of oil and TC removal. In the filtration system presented here, using ceramic hollow fiber ultrafiltration (UF) membranes with a d_{90} pore diameter of 40 nm, the removal of oil and TC from samples of tank dewatering produced water and oily model systems, was successfully demonstrated with a remarkable decontamination efficiency of >99.5% (oil) and 61–94% (TC), respectively.

*Corresponding author.

*Presented at the Conference on Desalination for the Environment: Clean Water and Energy
11–15 May 2014, Limassol, Cyprus*

1944-3994/1944-3986 © 2014 Balaban Desalination Publications. All rights reserved.

Keywords: Ceramic hollow fiber membranes (CHFMs); Produced water (PW) Treatment; Cross-flow velocity; Membrane fouling; Oil and total carbon (TC) removal efficiency

1. Introduction

1.1. Subject-produced water

Water is an integral part of process operations in many industries and increasing demand for water for industrial uses will result from increasing economic activity [1]. The same also applies to oil and gas exploration processes, which every year generate tremendous amounts of so-called “Produced Water” (PW) as a major by-product/waste stream associated with oil and gas production operations worldwide. PW is defined as any fossil water from underground formations that is brought to the surface during oil or gas manufacturing processes. It is considered to be one of the largest waste streams associated with oil and gas production and is often mixed with make up or source water [2]. PW from offshore and onshore oil and gas exploration, resulting from drilling and production operations, is a continuous source of contaminants to ecosystems [3]. Its treatment and management are growing challenges in all oil and gas producing regions. Currently, there are two main approaches recommended for the management of PW: reinjection into the discharged wells and treatment for reuse. In this context, more than 60% of the generated PW is re-injected into the wells. PW reinjection and drilling fluid recycling typically first require the removal of oil and suspended solids [4].

The composition of PW is very complex. Its characteristics and physical properties usually vary significantly depending on the geographic location of the field and the type of hydrocarbon product being produced [3]. It often contains different amounts of dispersed oil, dissolved organic compounds, production chemicals, corrosion products, heavy metals, large amounts of organic material, inorganic salts, and natural radioactive minerals. In the production phase, three barrels of PW are generated for every corresponding barrel of oil produced [4,5]. This ratio increases as oil wells mature and may reach as many as 7–10 barrels of PW per oil barrel, especially in mature oilfields [6]. Alzahrani et al. [7] estimated that given the oil production in 2011 (around 72,000,000 bbl/d), and the minimum ratio of 3 barrels of PW for each barrel of oil produced, a minimum of around 216,000,000 bbl/d of PW was generated in 2011 alone. This large quantity of PW is mainly reused by

re-injecting into the well or else discharged into the environment. Due to this huge amount of PW generated, its management has become a major issue for the public and regulators [8]. The large volume of PW presents not only environmental challenges, but also potential opportunities for beneficial reuse, recycling, and disposal alternatives [9]. Thus, it is absolutely necessary to improve innovative technologies of PW treatment in order to not only meet the increasingly stringent environmental regulations, but also to improve the economic viability of the processes [10] and possibly lead to a new source of water.

1.2. Technologies for PW treatment

Currently, the objectives of PW treatment technologies include deoiling, desalination, degassing, suspended solids removal, and organic compounds removal. The common process techniques used for the pre-treatment of PW are sand filtration, sedimentation, gas flotation, hydrocyclones, and separators [11]. One of the main goals of any treatment process for PW is a significant reduction in the level of dispersed hydrocarbons and suspended solids in the wastewater [12]. In the past few decades, various technologies including biological [13,14], physical [15], and chemical [16] treatment processes or a combination of these [13,17] have been developed and investigated for the treatment of oilfield PW. Among these technologies, a significant amount of research has been conducted in the field of PW treatment using microfiltration (MF), ultrafiltration (UF), nanofiltration (NF), reverse osmosis (RO), membrane distillation (MD), and their combined processes using different types of membranes [7,18,19]. Ahmadun et al. [20] give an overview on different facets of membrane technology used for PW treatment. In a series of research papers, the authors have previously described that membrane separation technology offers a potential application in the processing of oilfield PW [21–25]. Major technical challenges that are associated with the integration of membrane processes for more effective PW treatment include: high filtrate flux and quality, low-fouling properties, easy cleaning, chemical stability, and thermal stability. Ceramic membranes have been developed and used in a variety of different applications, especially where harsh process conditions (e.g. physical

and chemical properties of feed solution or high temperature and pressure operation) preclude the current practice of using polymeric membranes. In this context, the application of tubular and rotating ceramic membranes has been proposed as a promising technology for treatment of oilfield PW. Ceramic hollow fiber membranes (CHFMs) represent a new generation in the development of inorganic membranes by offering the advantages of one membrane consisting of both inorganic material and hollow fiber geometry. CHFMs, as they are used in this study, show some advantages and characteristic properties compared with other types of hollow fiber membranes (see Section 2.3).

Among other advantages [26,27], they have a larger surface area for filtration with the same volume of the membrane module (in comparison with tubular membranes), due to the higher number of channels [28]. In this study, the efficient treatment of oilfield PW generated from tank dewatering produced water (TDPW) and oily model systems (OMS) was studied using an innovative ultrafiltration CHFMs with a d_{90} pore diameter of 40 nm. In a first test series, the effect of cross-flow velocity (CFV) on the CHFMs performance as well as the highest possible permeate quantity and quality was investigated in terms of membrane fouling behavior, efficiency of oil and total carbon (TC) removal, and membrane cleaning effectiveness at a constant low trans-membrane pressure (TMP) of 0.5 bar and a constant process temperature of 40 °C.

2. Ceramic hollow fiber membranes

The most important membrane material and application characteristics of ceramic membranes are:

- (1) High chemical and thermal stability, which allows filtration of acids, bases, solvents, and hot media as well as cleaning under harsh conditions.
- (2) High mechanical stability during the filtration of abrasive media.
- (3) Low-fouling risk and adhesion potential for molecular organic substances.
- (4) Very clean membrane after production (sintering process).

CHFMs in particular offer further advantages compared with other ceramic membrane geometries such as multi-channel elements or ceramic disk membranes:

- (1) High packing density (high ratio of membrane surface/filter volume).

- (2) Defined flow conditions especially in the in-out cross-flow filtration mode.
- (3) Low material costs with respect to filter area.
- (4) Low sintering energy costs and time due to low membrane thickness.

The CHFMs that were used for the previously described experiments are manufactured by a simultaneous spinning and phase inversion process. In the next Section 2.1., this manufacturing process is presented. A descriptive physical model is explained in Section 2.2. which correlates operational and material parameters of the spinning and phase inversion process to the structure of the CHFMs. Finally, the design concept and the advantages of the two-layer membrane structure that was utilized in the experiments are delineated.

2.1. Spinning and phase inversion process

CHFMs are produced starting with the raw materials of ceramic and polymeric granular powder, an adequate solvent system, and some additive ingredients. These components are mixed homogeneously, and the viscosity of the resulting liquid single-phase spinning dope is a significant quality parameter that gives an indication of the properties of the subsequently produced hollow fiber membranes. The spinning dope is pressed through a two-component nozzle into an aqueous precipitation bath (“spinning process”) where the solid structure of the hollow fiber membrane is developed from the liquid spinning dope by phase inversion. In detail, the solvent is washed out from the spinning dope by the water within the precipitation bath. As the polymeric component is not soluble in water, it becomes a solid structure, which then generates the hollow fiber membrane. This so-called green fiber shows polymeric characteristics and it comprises singular embedded ceramic particles. The green fiber is further washed and then sintered at high temperatures. During the sintering process, the polymeric component is burned completely and the ceramic particles combine with each other forming sinter necks between the single particles. In the end, a pure CHFMs is generated. This CHFMs has smaller dimensions in comparison with the green fiber due to thermal shrinkage. In Fig. 1, the phase diagram of the three-component system polymer/solvent/water is shown qualitatively.

The white area indicates the region where all components within the spinning dope are miscible (single-phase region). Within the blue section, the components are immiscible. The spinning process

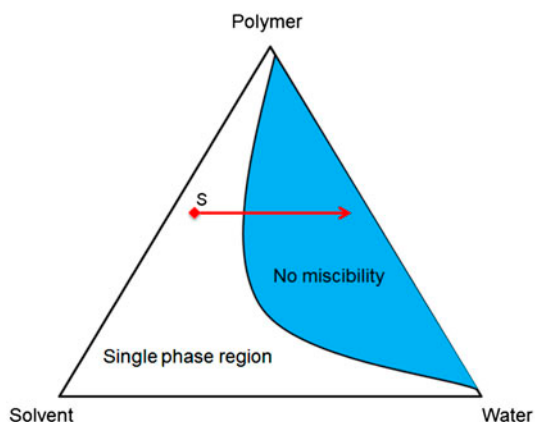


Fig. 1. Phase diagram of the polymer/solvent/water system with stable (single-phase region) and unstable (immiscible) region and process trajectory of the precipitation process.

starts at a state within the white area (point S) and as the spinning dope is brought into contact with the precipitation fluid (water) in the precipitation bath, the water penetrates the spinning dope. Within this step, the boundary line is crossed which separates the stable single-phase region from the unstable immiscible system state. Within the immiscible region, the solid green fiber is generated by precipitation.

Fig. 2 shows the orifice cross-section of the two-component spinning nozzle. The outer annular cross-section is driven through the spinning dope. In the inner circular cross-section, the bore fluid, which is also usually water or an aqueous solution, is conducted. The bore fluid is brought into contact with the spinning dope only at the nozzle orifice so a pre-precipitation is avoided. The nozzle orifice itself is either positioned at a very small distance (spinning with air gap) over the precipitation bath or it is dipping directly into the precipitation bath.

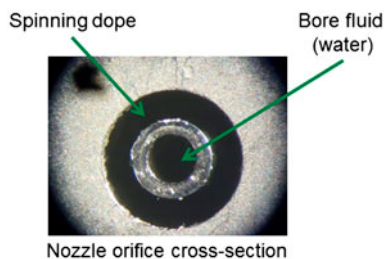


Fig. 2. Orifice cross-section of a two-component spinning nozzle with annular cross-section (conduction of spinning dope) and central circular cross-section (conduction of bore fluid).

2.2. Physical model to describe the formation of fiber structures

The main characteristic parameters of the CHFMs are the pore sizes and the pore structure which can be symmetric or asymmetric. The pore morphology varies between a cellular (sponge) structure with regular cells and a finger pore structure with elongated pores. With the cellular structure, an increased mechanical stability is achieved, but the water flux is lower in comparison with a membrane with a finger pore structure. In Fig. 3, SEM photographs are shown from membranes with both structures.

The kinetics of the phase inversion process depends on the composition of the spinning dope and the replacement of the solvent by the water in the precipitation bath according to the phase diagram in Fig. 1. By increasing the concentration of the precipitation fluid (water) and simultaneous reduction of the solvent concentration in the spinning dope, the precipitation process is initiated. The kinetics of this phase inversion process determines the morphology of the CHFMs. In the literature, some parameters are investigated which promote the generation of a cellular (foam) membrane structure in polymeric hollow fibers [29]. The main impact parameters are the polymer concentration, the viscosity of the spinning dope, and the solvent concentration within the precipitation bath. The formation of the cellular pore structure can be described by the diffusion-driven exchange of the solvent by the precipitation fluid (water) [30]. The diffusion starts when the spinning dope comes into contact with the precipitation fluid (water). The diffusion velocity of water molecules into the spinning dope is much higher than the diffusion velocity of the solvent molecules out of the spinning dope into the precipitation bath. This is due to the lower hydrodynamic radius of the water molecules compared with the solvent molecules. In this case, the fiber swelling, combined with the formation of macrovoids, results in finger pores. By deceleration of the diffusion process of the precipitation fluid into the spinning dope, the formation of macrovoids is suppressed and the cellular foam structure, which remains due to the homogeneous distribution of the polymeric component and the ceramic particles in the spinning dope, is preserved during the phase inversion. Both diffusion processes and the resulting fiber structures are shown schematically in Fig. 4.

A qualitative estimation of the diffusion flux can be done by the theoretical approach presented by Fick. The diffusion flux j depends on the diffusion coefficient D , the fluid density ρ and the concentration gradient $\frac{\partial c}{\partial x}$ of the diffusing species (here: water and solvent).

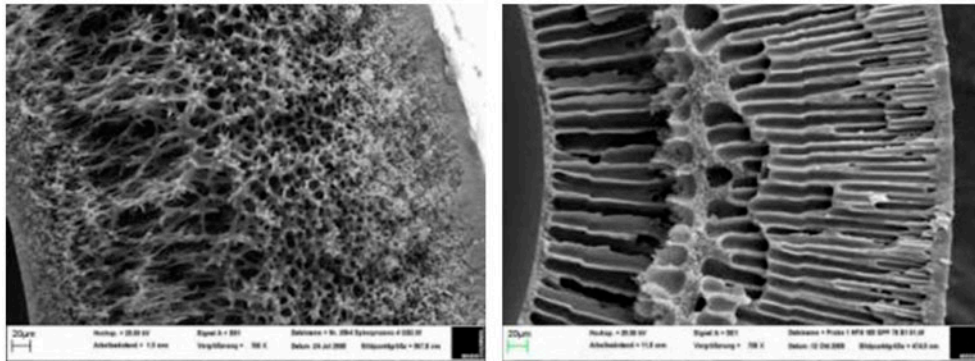


Fig. 3. SEM photos of CHFMs with cellular (sponge) pore structure (left) and finger pore structure (right).

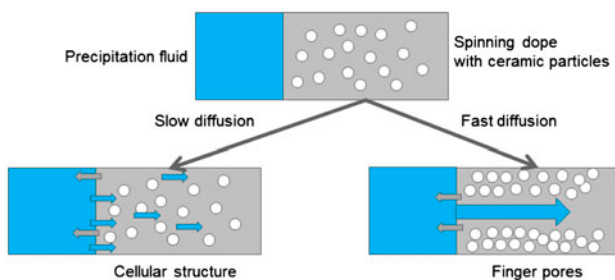


Fig. 4. Physical model to describe differences in the formation of a cellular structure and a finger pore structure in CHFMs by diffusion interactions between precipitation fluid and solvent.

$$j = -D\rho \frac{\partial c}{\partial x}$$

This is a simplification of the reality, because Fick's law describes single-component diffusion whereas the real diffusion process in this case is a multi-component diffusion. However, with Fick's law, it is shown that an increase of the solvent concentration in the precipitation bath lowers the driving concentration gradient for the solvent molecule diffusion out of the spinning dope.

The diffusion velocity can be estimated by the diffusion coefficient D , according to Stokes–Einstein in liquids:

$$D = \frac{k_B T}{6\pi\mu R_h}$$

Here, k_B is the Boltzmann parameter ($k_B = 1.381 \times 10^{-23}$ J/K), T is the absolute temperature (in K), μ is the dynamic viscosity of the fluid (in Pas), and R_h is

the hydrodynamic radius of the fluid molecule (in m). A temperature increase of the precipitation bath shows a double effect on a higher diffusion flux. First, the diffusion coefficient increases directly with temperature. Second, the dynamic viscosity of the precipitation bath decreases with temperature which also results in an increased diffusion flux. A viscosity increase of the precipitation bath induces a reduced diffusion in flux.

2.3. Specific design of the used CHFMs

The CHFMs, which were used in the experiments, consist of a two-layer structure. The ceramic microfiltration support layer with open pores and low-pressure drop results from the previously described spinning (precipitation) process and gives the mechanical stability to the membrane. After sintering, this support layer is covered by a functional ultrafiltration ceramic coating layer (active layer) on the feed side of the membrane. As the current membranes are operated in an in–out filtration mode, the coating is applied on the inner lumen surface of the hollow fiber membrane. For this coating process, the hollow fiber channel is flushed with a ceramic suspension, which adheres as a thin layer to the support layer. After flushing, the CHFMs are sintered a second time to achieve a stable bond between the ceramic coating and the support layer.

With this membrane design, the active coating layer has a thickness of only a few micrometers. This membrane design leads to a low TMP in operation and to a high permeate flux meaning the pressure drop of the open-structured support layer can almost be neglected.

In Fig. 5, this specific membrane structure is shown schematically. Fig. 6 shows the active coating and the support layer with two SEM photos.

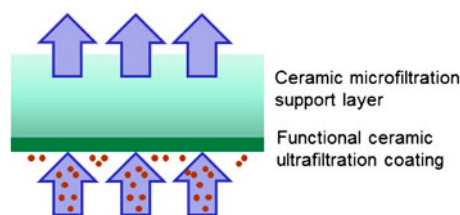


Fig. 5. Schematic representation of the design of the CHFMs applied within the experiments with the ceramic microfiltration support layer and the functional ceramic ultrafiltration coating layer (active layer).

3. Material and methods

3.1. CHFMs filtration system

The filtration experiments were carried out in cross-flow mode with ceramic hollow fiber ultrafiltration membranes (Table 1, Fig. 7) with in/out filtration direction. These membranes have a d_{90} pore diameter of 40 nm (MANN + HUMMEL GmbH, Ludwigsburg, Germany).

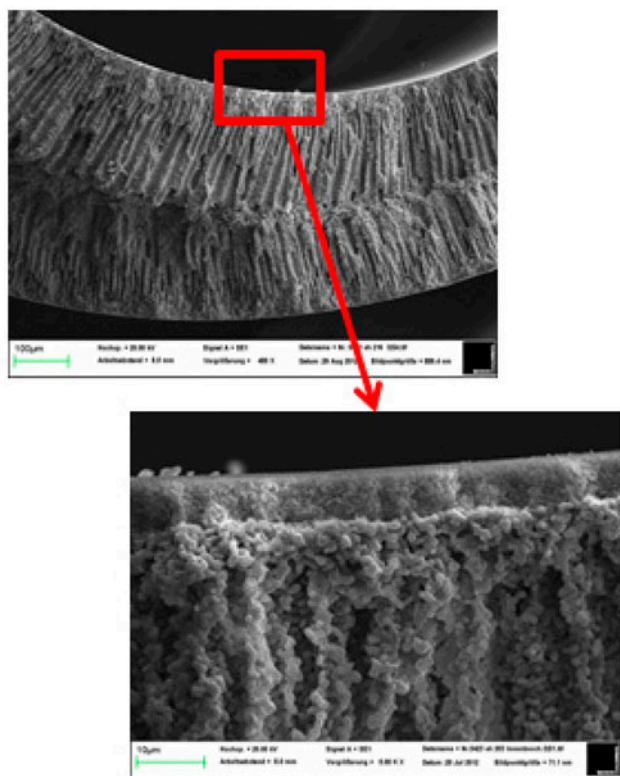


Fig. 6. SEM photos of the CHFMs utilized within the experiments showing the ceramic microfiltration support layer and the ceramic functional ultrafiltration coating layer (active layer).

The filtration system (Fig. 8) comprises the centrifugal pump, the CHFMs unit, the feed stream, permeate stream and retentate stream ducts (maximum operating pressure and temperature of 3 bar and 80 °C), and the back-flushing unit with a maximum operating pressure of 10 bar.

During the experiments, the CFV was varied, while the other parameters were kept constant. The filtrations were conducted optionally in fed-batch and total recycle mode, respectively. As needed, back-flushing was executed by pumping a mixture of permeate and air at regular time intervals, in the reverse out/in direction. The mean TMP was determined by measuring the pressure before and after the CHFMs module and averaging these values. All filtration experiments were carried out at a process temperature of 40 °C, a low TMP of 0.5 bar, and at an initial oil concentration in TDPW and the OMS of 1,000–5,200 ppm and 35 ppm, respectively. The permeate flow was measured with an electronic balance (DS 36K0.2, Kern, Germany) connected to a supervisory control and data acquisition system (Hitec Zang, Herzogenrath, Germany). The membrane was chemically cleaned after each filtration experiment with a 1% P3 Ultrasil-14 cleaning solution (Henkel, Düsseldorf, Germany). After the cleaning process, the clean water permeability of the membrane was measured and the cleaning process was repeated until the initial permeability of the membrane was achieved.

3.2. Oily wastewater quality analyses

The continuous oil-in-water measurement down to part per million (ppm) levels was performed using an online monitoring device, developed for industrial applications (DECKMA HAMBURG GmbH, Hamburg, Germany). Using a multi-range conductivity meter (HI 9033, Hanna Instruments, Kehl am Rhein, Germany), the electric conductivity in feed and permeate was determined. All samples were analyzed for TC with a TOC-V, Total Organic Carbon Analyzer (Shimadzu, Duisburg, Germany). Offline determination of the dispersed oil content was performed with TD500D an oil-in-water meter based on fluorescence measurement (Nordantec, Bremerhaven, Germany).

3.3. Oily wastewater characteristics

Samples of TDPW were obtained from German BP AG, Oil Refinery Emsland, Lingen. OMS were prepared by pre-emulsification of a crude oil (oilfield Bramberge, Germany) with a rotor stator homogenizer and subsequent processing with an Emulsiflex C5

Table 1

Properties of the hollow fiber ceramic ultrafiltration membrane and modules used in the filtration of OMS

d_{90} pore diameter	Active layer	d_{in}	d_{out}	Number of hollow fibers	Module length	Filtration area
40 nm	Al_2O_3	2 mm	4 mm	30	26 cm	0.037 m ²
40 nm	Al_2O_3	2 mm	4 mm	100	45 cm	0.25 m ²

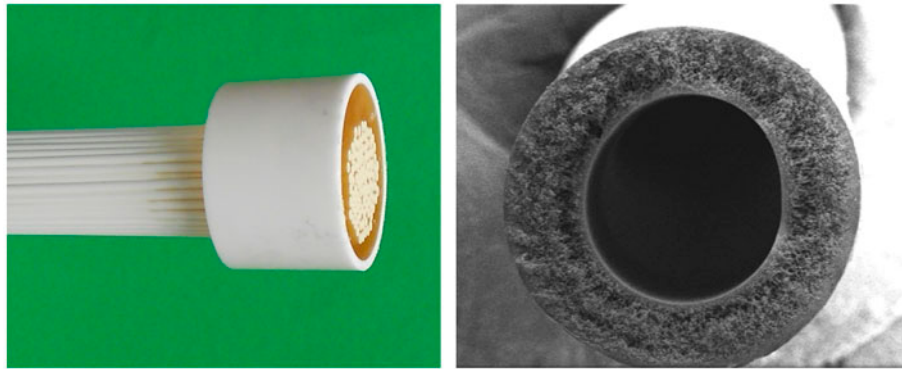


Fig. 7. Photos of the CHFMs used in this study (fiber bundle with potting (left) and single CHFMs (right)).

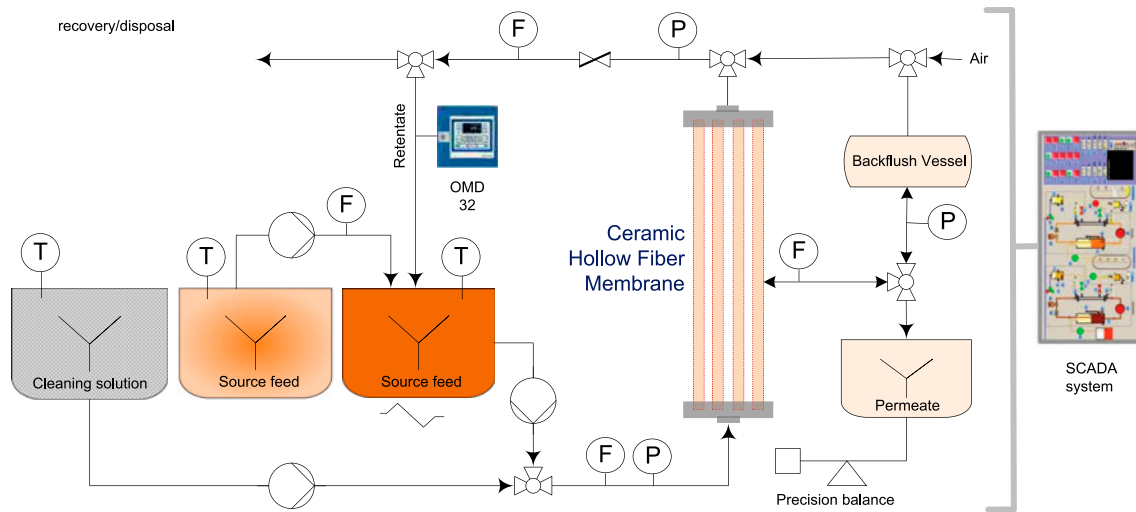


Fig. 8. Schematic diagram of the laboratory-scale CHFMs system in fed-batch and/or total recycle mode.

high-pressure homogenizer (Avestin, Mannheim, Germany) at 450 bar in single pass.

The final concentration of dispersed oil in OMS was adjusted to 35 ppm by dilution with demineralized water while circulating the OMS through the OMD 32 oil monitoring device. A summary of components and their ranges of concentrations in TDPW and OMS used in this study are given in Table 2.

4. Results and discussions

During the treatment of oily wastewaters using membrane technology, there are several mechanisms and factors that cause and influence membrane fouling, such as, physical and chemical characteristics of the oily wastewater (concentration of oil and other solutes materials in feed solution, particle size, and nature of components), hydrodynamic operating conditions (TMP, CFV, and process temperature),

Table 2
Physical parameters of TDPW and OMS feed samples at 40 °C

Index	Unit	OMS	TDPW
Dispersed oil	mg l ⁻¹	30–200	200–5,000
pH	–	6.2–6.9	6.0–8.0
Conductivity	μS	8.3–	20,000–
	cm ⁻¹	15.7	80,000
Viscosity	mPa.s	0.6–0.7	1.1
COD	mg l ⁻¹	105–	1,000–9,900
		169	
TC	mg l ⁻¹	50–658	200–5,000

properties of membrane used (pore size, pore size distribution, hydrophilicity, and membrane material), and the possible interactions between membrane and foulants [21–25]. Since membrane fouling, caused by the deposition of particles on the membrane pores, within the membrane pores or onto the surface, affect the membrane permeability and reduce the efficiency during the treatment of wastewaters [31], variation of operating conditions in cross-flow filtration processes can be a useful technique in investigating their effects on the fouling behavior of membranes and their permeate flux. Generally, the variation of the relevant process parameters, such as TMP, CFV, and temperature can have an influence on the separation performance and permeate quality of a given membrane [32]. Therefore, in this study and in a first test series, the effect of CFV on the CHF performance, as well as the highest possible permeate quantity and quality, was investigated during the treatment of TDPW and OMS. The tests focused on membrane fouling behavior, efficiency of oil and TC removals, and membrane cleaning effectivity at a constant low TMP of 0.5 bar and a constant process temperature of 40 °C.

4.1. Effect of CFV

The effect of CFV on the permeate flux over time during the treatment of TDPW is shown in Fig. 9. No back-flushing or chemical cleaning step was applied within the considered testing time. The CFV variation ranges from 1.5 m s⁻¹ over 2.0 m s⁻¹ to 2.5 m s⁻¹ corresponding to Reynolds numbers from 2,900, 3,800, and 4,800 referring to the lumen side of the CHF, which indicate turbulent flow. Figs. 9 and 10 also show that at the beginning of the TDPW filtration experiments, the increase in CFV from 1.5 to 2.5 m s⁻¹ caused a percentage increase in the initial permeate flux of up to 75% (from 110 to 191 l m⁻² h⁻¹) and lead to a higher

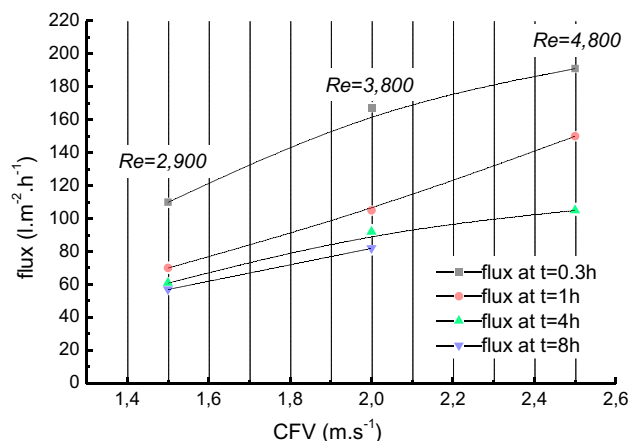


Fig. 9. Comparison of permeate flux for a 40 nm CHF and TDPW at different cross-flow velocities (1.5, 2.0 and 2.5 m s⁻¹) over time; TMP 0.5 bar; temperature 40 °C; oil content 1,000 ppm.

steady permeate flux during treatment of TDPW. This indicates that high CFV can enhance the permeated flux, which could be explained by the change of Reynolds number. Re is defined as follows:

$$Re = \frac{\rho v d}{\mu}$$

where ρ is the density of the liquid, v the mean velocity of the liquid in the hollow fiber lumen, d the lumen diameter of the CHF, and μ is the dynamic viscosity of the liquid. The oil and TC removal efficiencies under various applied CFV values were

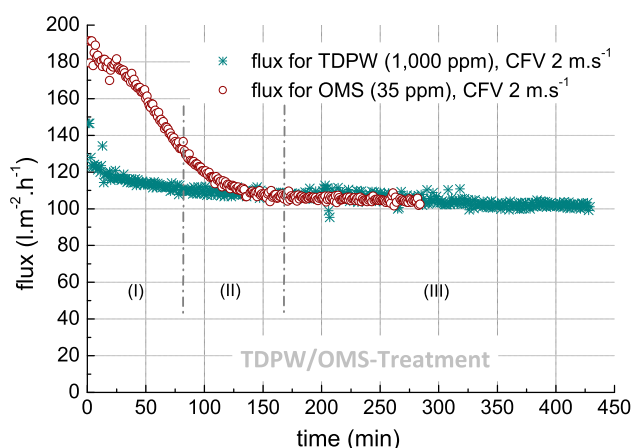


Fig. 10. Comparison of permeate flux variation for a 40 nm CHF over time for TDPW and OMS; CFV 2 m s⁻¹; TMP 0.5 bar; temperature 40 °C.

always maintained around 99.9% and between 61 and 94%, respectively.

Fig. 10 shows a representative flux–time curve of the ceramic hollow fiber ultrafiltration membrane used in this study during the treatment of different types of oily wastewaters (TDPW and OMS) with the same process parameter and without any changes in the running treatment process (e.g. back-flushing).

It starts with (I) an initial drop in the permeate flux caused by membrane fouling, depending on the properties of the feed and process parameters applied, which is (II) followed by a reasonably long/short period of gradual flux decrease that exhibits varied intensity and duration, and (III) ends with a steady-state flux.

The flux decline vs. time throughout the ultrafiltration process of OMS for two different CFVs (1.6 and 2.5 m s^{-1}) is illustrated in Fig. 11.

The CHFMs used in this study demonstrated an initial permeate flux of $1901 \text{ m}^{-2} \text{ h}^{-1}$ when operated at a CFV of 2.5 m s^{-1} and reached a quasi-stable performance of $1001 \text{ m}^{-2} \text{ h}^{-1}$ within 3.5 h of the trial time. In this experiment, the permeate flux shows a decline of 43% within regions (I) and (II), when compared with the initial flux of $1901 \text{ m}^{-2} \text{ h}^{-1}$. In this case, and after a total running time of 5 h, an average permeate flux rate of around $1241 \text{ m}^{-2} \text{ h}^{-1}$ was achieved. Fig. 11 also clearly shows the effect of a lower CFV applied at 1.6 m s^{-1} on the membrane performance which results in a remarkable shift of limiting flux regions (II) and (III), when compared with the experiment with a higher CFV of 2.5 m s^{-1} during the treatment of OMS. After 4.5 h of filtration time, within the regions (I) and

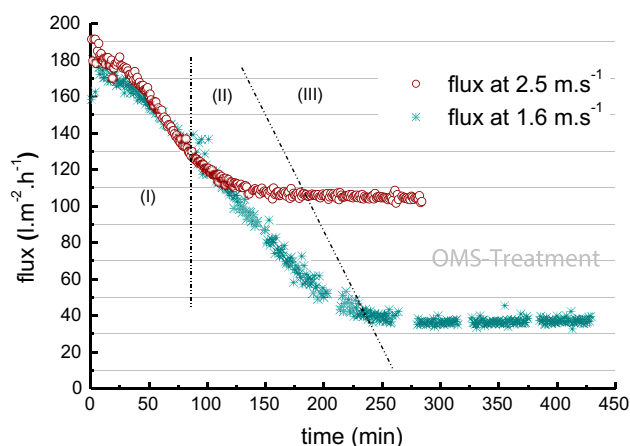


Fig. 11. Comparison of permeate flux variation for a 40 nm CHFMs with time for OMS at different CFV 1.6 and 2.5 m s^{-1} ; TMP 0.5 bar; temperature 40°C .

(II), a decline in permeate flux of 76% was observed. During a running time of 5 h, the average permeate flux rate was found to be $971 \text{ m}^{-2} \text{ h}^{-1}$. In Fig. 12, the variation of normalized flux over time for a 40 nm CHFMs for the treatment of TDPW in fed-batch mode at three different cross-flow velocities (1.5, 2.0, and 2.5 m s^{-1}) and a low TMP of 0.5 bar is shown. The normalized flux J_n was calculated from:

$$J_n = \frac{J_t}{J_{cw}}$$

where J_t is the permeate flux at time t and J_{cw} is the clean water permeability.

As seen in Fig. 12, the effect of CFV on permeate flux was more pronounced at the lowest CFV of 1.5 m s^{-1} compared with higher CFVs of 2.0 and 2.5 m s^{-1} . The oil content in the different real TDPW batches used varied between 1,000 and 2,000 ppm in the feed fluxes. The membrane filtration performed at a CFV of 2.5 m s^{-1} was characterized by the highest initial and steady-state permeate fluxes, and by the lowest decline in the normalized flux caused by the larger hydrodynamic shear forces at higher CFV that probably removed the foulants.

The normalized flux declined to 61, 28, and 25% of the initial normalized flux after 100 min of operation, for 1.5, 2.0, and 2.5 m s^{-1} , respectively. This in turn increases the filtration efficiency as a result of the thinner fouling layer associated with higher CFV. These results are consistent with those of other studies that attributed the increase in membrane permeability

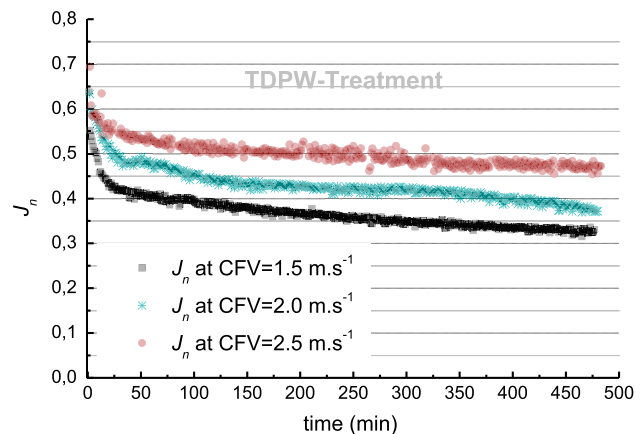


Fig. 12. Variation of normalized membrane flux for a 40 nm CHFMs and TDPW as a function of operating time and different cross-flow velocities, 1.5 m s^{-1} ($C_{oil} = 1,800 \text{ ppm}$), 2.0 m s^{-1} ($C_{oil} = 2,000 \text{ ppm}$) and 2.5 m s^{-1} ($C_{oil} = 1,000 \text{ ppm}$); TMP 0.5 bar; temperature 40°C .

and decrease in membrane fouling with CFV increase to higher levels of turbulence [23–25,33,34]. The results shown in Fig. 12 indicate that membrane fouling of different applied CFVs produce different fouling situations and trends. The effect of CFV on the permeate quality over the test duration of 8 h was evaluated by determining oil and TC concentration in permeate samples. Here again, over the entire duration of the filtration experiments, a significant oil removal efficiency of more than 99.5% could be observed in all permeate samples at any applied CFV.

4.2. Mean and long-term ultrafiltration of PW

The flux decline over the filtration time, as an unavoidable phenomenon in the MF and UF processes, is mainly related to the membrane fouling (reversible or irreversible), which may be the combined effects of the formation of a cake layer on the membrane surface and/or membrane pore blockage [35,36]. With the objective to observe and evaluate the CHF performance over a long filtration period of several days, the cross-flow filtration system was set to total recycle mode, with and without back-flushing, to treat TDPW at a constant low TMP of 0.5 bar. The change in the permeate flux for a ceramic hollow fiber UF-membrane and two different oil concentrations in TDPW (TDPW1 = 5,200 ppm and TDPW2 = 2,100 ppm) during two mean-term experiments for 30 h is shown in Fig. 13. Once the mean-term membrane filtration process begins, the permeate flux reaches its steady state, typically, after a certain time period depending on the applied process parameters (e.g. CFV) as well as the concentration of foulants in the TDPW. The results indicate that the continuous accumulation of suspended materials in TDPW, and retained particles on the membrane surface, results in forming a compact cake layer, which increasingly restricts membrane permeability.

A comparison of different observed flux trends for TDPW1 and TDPW2 at the same CFV of 2.0 m s^{-1} and TMP of 0.5 bar for a trial duration of around 17 h shows that the flux decline could be a result of different degrees of pore blockage and/or cake layer formation. Higher average permeate flux was obtained at a lower initial oil concentration. During the experiment with TDPW2 and an initial oil concentration of 2,100 ppm, the flux declined within the first 2 h from the starting value of $140 \text{ l m}^{-2} \text{ h}^{-1}$ before reaching a fairly stable but slightly declining permeability for the remaining 400 min of filtration. After 17 h of total filtration time, the level of flux reached $80 \text{ l m}^{-2} \text{ h}^{-1}$ and remained almost constant until the end of the

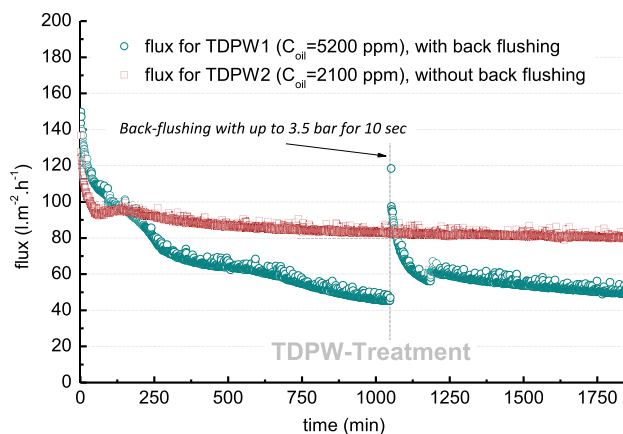


Fig. 13. Mean-term membrane filtration performance flux for a 40 nm CHF membrane over time at CFV of 2.0 m s^{-1} and different initial oil concentrations in TDPW1 (5,200 ppm) and TDPW2 (2,100 ppm) with and without back-flushing; TMP 0.5 bar; temperature 40°C .

experiment. Fig. 13 also shows a representative example of the results obtained with TDPW1 and a high initial oil concentration of 5,200 ppm. According to this figure, the water permeability of the UF membrane decreases continuously within the first 4 h due to membrane fouling, from the initial value of $143 \text{ l m}^{-2} \text{ h}^{-1}$ and after that falling to around $45 \text{ l m}^{-2} \text{ h}^{-1}$ over the remaining 12 h. So for the operating conditions for TDPW1 = 5,200 ppm, a mechanical back-flushing step was performed after about 1,050 min. to increase the flux. Permeate water was pressed through the membrane from the outside to the inside against the filtration direction at a TMP of 3.5 bar for 10 s. It can be seen from the diagram that the original flux value was achieved by about 75% with this simple mechanical cleaning step.

Back-flushing under optimized operating conditions and provision of high cross-flow velocities are some of the useful strategies that can be incorporated to reduce or control membrane fouling [36]. It should be noted that the effective control of membrane fouling in MF/UF processes could be dependent on the mode and effectivity of back-flushing. Several pilot studies demonstrated that an increase in back-flushing frequency and duration significantly reduced membrane fouling [37]. Therefore, in this study, the effectiveness of rapid back-flushing in enhancing the permeate flux in cross-flow ultrafiltration of PW has been demonstrated. In order to reduce the impact of fouling on membrane performance, a long-term UF of TDPW with a CHF membrane and a high oil concentration of 5,200 ppm was investigated, which employed back-flushing over a test duration of 9 days (Fig. 14).

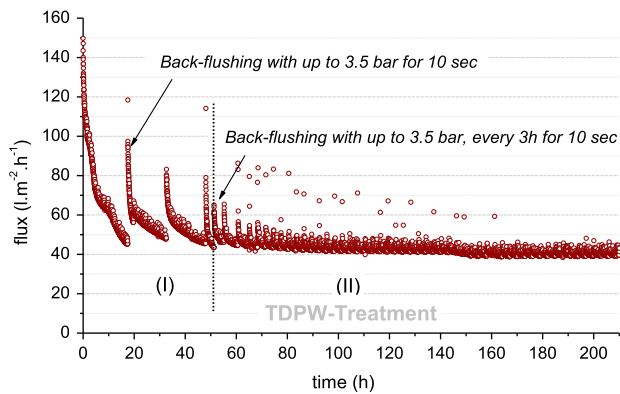


Fig. 14. Long-term membrane filtration performance flux for a 40 nm CHFMs and TDPW over time; CFV 2.0 m s^{-1} ; TMP 0.5 bar; temperature 40°C , oil concentration 5,200 ppm.

4.3. Effect of the back-flushing

The permeate flux of the CHFMs was measured as a function of filtration time of 9 days using TDPW with an oil concentration of 5,200 ppm. As shown in Fig. 14, the permeate flux declined from the initial $149 \text{ l m}^{-2} \text{ h}^{-1}$ after 1-h running time at a CFV of 2.0 m s^{-1} and a TMP of 0.5 bar. The reduction in permeate flux continued within the next 15 h to a level of $46 \text{ l m}^{-2} \text{ h}^{-1}$. In order to limit the minimum permeate flux at 30%, compared with initial membrane permeate flux, two back-flushing modes with different frequencies were chosen: (I) back-flushing with up to 3.5 bar for 10 s. every 18 h and (II) back-flushing with 3.5 bar for 10 s, every 3 h. When the back-flushing was performed, a rapid increase in the permeate flux of up to $118 \text{ l m}^{-2} \text{ h}^{-1}$ was observed in region (I), which corresponds to a regeneration of permeate flux of up to

Table 3
Summary of results derived from 40 nm CHFMs

d_{90} pore diameter	Feed type	Filtration mode	Duration	TMP (bar)	CFV (m s^{-1})	C_{oil} in retentate at t_0-t_{end} (ppm)	Oil-removal (%)	C_{TC} (ppm)	TC-removal (%)
40 nm	TDPW	TRM	LT	0.5	2.0	4,600	>99.5	N.A.	N.A.
40 nm	TDPW	TRM	LT	0.5	2.0	5,200	>99.5	N.A.	N.A.
40 nm	OMS	FBM	MT	0.5	1.5	59	>99.5	56	94
40 nm	TDPW	FBM	MT	0.5	1.5	1,800–14,000	>99.5	2,894	61
40 nm	TDPW	FBM	MT	0.5	2.0	2,500–19,000	>99.5	3,183	76
40 nm	TDPW	FBM	MT	0.5	2.5	3,000–30,000	>99.5	3,222	80

Note: TRM: Total recycle mode; FBM: Fed-batch mode; LT: Long-term; MT: Mean-term; TDPW: Tank dewatering produced water; OMS: Oily model systems.

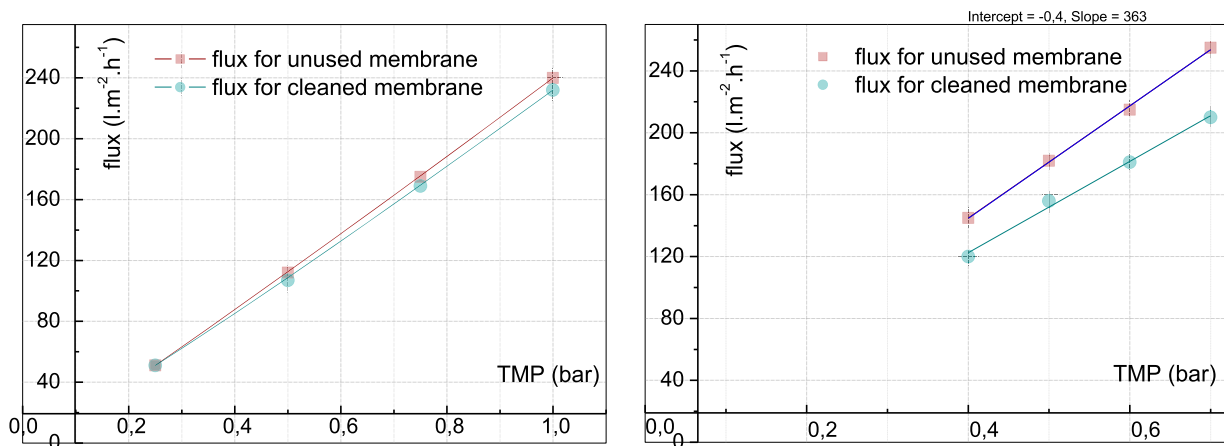


Fig. 15. Comparison of clean water fluxes of unused and cleaned CHFMs (left) after a short-term test and (right) long-term test and subsequent cleaning procedure with alkaline cleaning agent.

80% compared with the initial permeate flux. In region (II) with the back-flushing parameter applied, the level of flux reached $40 \text{ l m}^{-2} \text{ h}^{-1}$ and remained almost constant until the end of the experiment. The results of these experiments have shown that rapid back-flushing can be temporarily effective during the treatment of PW containing high oil concentrations, and its effectiveness declines with increasing trial duration.

4.4. Oil and TC rejection efficiency

Besides the permeate membrane flux, rejection is another important parameter to represent membrane performance. The values of oil and TC removals obtained from six representative experiments are reported in Table 3. It shows that the 40-nm ceramic hollow fiber UF membrane always gave an excellent oil rejection of higher than 99.5% for both OMS and TDPW, independent of the initial oil concentration of the feed. Also during the treatment of OMS with an initial TC concentration between 50 and 100 ppm, an efficient TC removal of 90–95% was achieved.

4.5. Clean water flux/chemical cleaning effectivity

Chemical cleaning of membranes is an integral part of operation for MF/UF systems in wastewater treatment and has significant impact on membrane performance. In this study, a series of filtration experiments were performed systematically to investigate the chemical cleaning effectivity of the CHFMs used. Therefore, prior each filtration experiment, the flux of pure water through the unused membrane was measured with distilled water at different TMP at room temperature. Additionally, after completing the chemical cleaning procedure for a fouled membrane, the clean water fluxes were also measured in the same way.

In Fig. 15, representative results of the clean water flux measurements as a function of TMP for a CHFM before and after two TDPW treatment processes (short-term test with a running time of 8 h and mean-term test over 70 h of running time), are shown. After the filtration and membrane cleaning with alkaline agents, the water permeability could be regenerated to 94% compared with the clean water permeability of the unused membrane (Fig. 15, left). A cleaning effectivity of 83% was observed after a mean-term filtration experiment of 70 h (Fig. 15, right), indicating that more permanent membrane fouling occurs during longer operation periods. All together, the results show that the chemical cleaning effectivities of the ceramic membranes fell between 70 and 100%, depending on the

operating conditions (test duration and applied CFV) during the treatment process.

5. Conclusions

PW, any fossil water that is brought to the surface along with crude oil or natural gas, is difficult to handle/treat and represents the largest volume of waste associated with the oil and gas industry.

Major technical challenges that are associated with the integration of any membrane processes for more effective PW treatment include: high filtrate flux and quality, low-fouling properties, easy cleaning, chemical, mechanical, and thermal stability. In this research study, the efficient treatment of oilfield PW, generated from TDPW and OMS, was investigated using an innovative ultrafiltration (UF) CHFMs with a d_{90} pore diameter of 40 nm. In this context, in a first test series, the effect of CFV as a main membrane operating condition was studied based on membrane fouling behavior, oil, and TC removal efficiency at a low TMP of 0.5 bar. Based on the results of the filtration experiments presented in this work, the new CHFMs is a robust solution for the treatment of oily wastewaters and can be an excellent and effective technology for deoiling and TC removal from oilfield PW.

During the treatment of TDPW and OMS, oil and TC removal efficiencies higher than 99.5 and 61–94% were achieved, at any applied CFV. The design of the CHFMs presented here combines the advantages of both inorganic material and hollow fiber geometry, and allows the utilization of compact CHFMs systems that could reduce the space and weight of installed equipment within harsh onshore/offshore operating environments. This membrane design also leads to a low TMP in operation and to a high permeate flux meaning the pressure drop of the open-structured support layer can almost be neglected. In this study, also the chemical cleaning effectivity and the effectiveness of rapid back-flushing in enhancing the permeate flux in cross-flow ultrafiltration of TDPW has been demonstrated. Results have shown high chemical cleaning effectivities between 70 and 100%, depending on the operating conditions during the treatment process. It was also found that rapid back-flushing can be temporarily effective during the treatment of PW containing high oil concentrations.

It was especially demonstrated that the applied ultrafiltration CHFMs is able to treat high feed oil concentrations of some thousand ppm within stable membrane operation. Currently, membrane-based ultrafiltration is mostly used as a final polishing step in PW treatment with a feed water concentration of

only few hundred ppm. The characteristic of these new CHFMs to stand also process conditions with much higher feed oil contents bears the attractive potential of reducing the required number of total process steps in PW treatment.

In order to optimize the PW treatment process, further investigations evaluating the effect of process parameters, such as initial feed oil concentration, CFV, TMP, and alternative properties of the membranes and statistical combinations of these parameters, are in progress.

Acknowledgment

The authors would like to thank Dipl.-Ing. Martin Müller, German BP AG, Oil Refinery Emsland, Lingen, Germany, for providing us with the TDPW.

References

- [1] UNESCO, Global Water Resources Under Increasing Pressure from Rapidly Growing Demands and Climate Change, According to New UN World Water Development Report, WWDR4—Background Information Brief, United Nations World Water Assessment Program, 2012, UNESCOPRESS.
- [2] Y. Folarin, D. An, S. Caffrey, J. Soh, C.W. Sensen, J. Voordouw, T. Jack, G. Voordouw, Contribution of make-up water to the microbial community in an oil field from which oil is produced by produced water re-injection, *Int. Biodeterior. Biodegrad.* 81 (2013) 44–50.
- [3] T. Bakke, J. Klungsoyr, S. Sanni, Environmental impacts of produced water and drilling waste discharges from the Norwegian offshore petroleum industry, *Mar. Environ. Res.* 92 (2013) 154–169.
- [4] B. Kose, H. Ozgun, M. Evren Ersahin, N. Dizge, D.Y. Koseoglu-Imer, B. Atay, R. Kaya, M. Altinbas, S. Sayili, P. Hoshan, D. Atay, E. Eren, C. Kinaci, I. Koyuncu, Performance evaluation of a submerged membrane bioreactor for the treatment of brackish oil and natural gas field produced water, *Desalination* 285 (2012) 295–300.
- [5] B. Bailey, M. Crabtree, J. Tyrie, J. Elphick, F. Kuchuk, C. Romano, L. Roodhart, *Water control, Oilfield Rev.* 12 (2000) 30–51.
- [6] J.A. Veil, M.G. Puder, D. Elcock, R.J. Redweik Jr, A White Paper Describing Produced Water from Production of Crude Oil, Natural Gas, and Coal Bed Methane, Argonne National Laboratory, Lemont, IL, 2004.
- [7] S. Alzahrani, A.W. Mohammad, N. Hilal, P. Abdullah, O. Jaafar, Comparative study of NF and RO membranes in the treatment of produced water—Part I: Assessing water quality, *Desalination* 315 (2013) 18–26.
- [8] D. Wandera, S.R. Wickramasinghe, S.M. Husson, Modification and characterization of ultrafiltration membranes for treatment of produced water, *J. Membr. Sci.* 373 (2011) 178–188.
- [9] J.E. Horner, J.W. Castle, J.H. Rodgers, A risk assessment approach to identifying constituents in oilfield produced water for treatment prior to beneficial use, *Ecotoxicol. Environ. Saf.* 74 (2011) 989–999.
- [10] P. Xu, J.E. Drewes, Viability of nanofiltration and ultra-low pressure reverse osmosis membranes for multi-beneficial use of methane produced water, *Sep. Purif. Technol.* 52(1) (2006) 67.
- [11] A. Fakhru'l-Razi, A. Pendashteh, L.C. Abdullah, D.R.A. Biak, S.S. Madaeni, Z.Z. Abidin, Review of technologies for oil and gas produced water treatment, *J. Hazard. Mater.* 170 (2009) 530–551.
- [12] D. Robinson, Oil and gas: Treatment of produced waters for injection and reinjection, *Filtr. Sep.*, 50 (4), July–August, 2013, 38–43.
- [13] G. Li, S. Guo, F. Li, Treatment of oilfield produced water by anaerobic process coupled with micro-electrolysis, *J. Environ. Sci.* 22(12) (2010) 1875–1882.
- [14] Q. Li, C. Kang, C. Zhang, Waste water produced from an oilfield and continuous treatment with an oil-degrading bacterium, *Proc. Biochem.* 40 (2005) 873–877.
- [15] F. Bayati, J. Shayegan, A. Noorjahan, Treatment of oil field produced water by dissolved air precipitation/solvent sublation, *J. Pet. Sci. Eng.* 80 (2012) 26–31.
- [16] S. Shokrollahzadeh, F. Golmohammad, N. Naseri, H. Shokouhi, M. Arman-mehr, Chemical oxidation for removal of hydrocarbons from gas-field produced water, *Procedia Eng.* 42 (2012) 942.
- [17] J.M. Younker, M.E. Walsh, Bench-scale investigation of an integrated adsorption-coagulation-dissolved air flotation process for produced water treatment, *J. Environ. Chem. Eng.* 2 (2014) 692–697.
- [18] A. Alkudhiri, N. Darwish, N. Hilal, Produced water treatment: Application of air gap membrane distillation, *Desalination* 309 (2013) 46–51.
- [19] E. Yuliwati, A.F. Ismail, T. Matsuura, M.A. Kassim, M.S. Abdullah, Effect of modified PVDF hollow fiber submerged ultrafiltration membrane for refinery wastewater treatment, *Desalination* 283 (2011) 214–220.
- [20] F. Ahmadun, A. Pendashteh, L.C. Abdullah, D.R. Awang Biak, S.S. Madaeni, Z.Z. Abidin, Review of technologies for oil and gas produced water treatment, *J. Hazard. Mater.* 170 (2009) 530–551.
- [21] M. Ebrahimi, O. Schmitz, S. Kerker, F. Liebermann, P. Czermak, Dynamic cross-flow filtration of oilfield produced water by rotating ceramic filter discs, *Desalin. Water Treat.* 51(7–9) (2013) 1762–1768, doi: [10.1080/19443994.2012.694197](https://doi.org/10.1080/19443994.2012.694197).
- [22] M. Ebrahimi, Z. Kovacs, M. Schneider, P. Mund, P. Bolduan, P. Czermak, Multistage filtration process for efficient treatment of oil-field produced water using ceramic membranes, *Desalin. Water Treat.* 42 (2012) 17–23.
- [23] P. Czermak, M. Ebrahimi, Multiphase cross-flow filtration process for efficient treatment of oil-field produced water using ceramic membranes, *Proceedings 7th Produced Water Workshop*, paper 5, April 29–30, 2009, Aberdeen, UK.
- [24] K. ShamsAshaghi, M. Ebrahimi, P. Czermak, Ceramic ultra- and nanofiltration membranes for oilfield produced water treatment—A mini review, *The Open Environ. J.* 1 (2007) 1–8.
- [25] M. Ebrahimi, K. Shams Ashaghi, L. Engel, P. Mund, P. Bolduan, P. Czermak, Investigations on the use of

- different ceramic membranes for efficient oil-field produced water treatment, *Desalination* 250 (2010) 991–996.
- [26] M. Lee, Z. Wu, R. Wang, K. Li, Micro-structured alumina hollow fiber membranes - potential applications in wastewater treatment, *J. Membr. Sci.* 461 (2014) 39–48.
- [27] X. Tan, K. Li, Inorganic hollow fiber membranes in catalytic processing, *Curr. Opin. Chem. Eng.* 1 (2011) 69–76.
- [28] I. Gaspar, A. Koris, Z. Bertalan, G. Vatai, Comparison of ceramic capillary membrane and ceramic tubular membrane with inserted static mixer, *Chem. Pap.* 65 (5) (2011) 596–602, doi: [10.2478/s11696-011-0045-y](https://doi.org/10.2478/s11696-011-0045-y).
- [29] K. Ohlrogge, K. Ebert, *Membranen: Grundlagen, Verfahren und Industrielle Anwendungen*, Wiley-VCH, Weinheim, 2006.
- [30] E.L. Cussler, *Diffusion: Mass Transfer in Fluid Systems*, Cambridge University Press, Cambridge, 2009.
- [31] Z. Cui, W. Peng, Y. Fan, W. Xing, N. Xu, Effect of cross-flow velocity on the critical flux of ceramic membrane filtration as a pre-treatment for seawater desalination, *Chin. J. Chem. Eng.* 21(4) (2013) 341–347.
- [32] E. Alventosa-deLara, S. Barredo-Damas, M.I. Alcaina-Miranda, M.I. Iborra-Clar, Ultrafiltration technology with a ceramic membrane for reactive dye removal: Optimization of membrane performance, *J. Hazard. Mater.* 209–210(492–500) 2012 27–29.
- [33] A. Alpatova, E. Kim, S. Dong, N. Sun, P. Chelme-Ayala, M.G. El-Din, Treatment of oil sands process-affected water with ceramic ultrafiltration membrane: Effects of operating conditions on membrane performance, *Sep. Purif. Technol.* 122 (2014) 170–182.
- [34] H. Chen, A.S. Kim, Prediction of permeate flux decline in cross-flow membrane filtration of colloidal suspension: A radial basis function neural network approach, *Desalination* 192 (2006) 415–428.
- [35] A. Reyhani, F. Rekabdar, M. Hemmati, A.A. SafeKordi, M. Ahmadi, Optimization of conditions in ultrafiltration treatment of produced water by polymeric membrane using Taguchi approach, *Desalin. Water Treat.* 51(40–42) (2013) 1–10, doi: [10.1080/19443994.2013.776505](https://doi.org/10.1080/19443994.2013.776505).
- [36] A. Abdelrasoul, H. Doan, A. Lohi, Mass transfer - advances in sustainable energy and environment oriented numerical modeling, in: H. Nakajima (Ed.), *Fouling in Membrane Filtration and Remediation, Methods*, InTech, ISBN 978-953-51-1170-2, Published: July 24, 2013 (Chapter 8).
- [37] S. Hong, P. Krishna, C. Hobbs, D. Kim, J. Cho, Variations in backwash efficiency during colloidal filtration of hollow-fiber microfiltration membranes, *Desalination* 17(x) (2005) 257–268.
- [38] T. Janus, P. Parneet, B. Ulanicki, Modelling and simulation of short and long term membrane filtration experiments, *Desalin. Water Treat.* 8 (2009) 37–47.